Acta Crystallographica Section B
Structural Science
ISSN 0108-7681

Deuterated γ-malonic acid: its neutron crystal structure in relationship to other polymorphs of aliphatic dicarboxylic acids

R. K. McMullan,[a]‡ W. T. Klooster[b,c] and H.-P. Weber[d]*

[a]Chemistry Department, Brookhaven National Laboratory, Upton, NY 11973, USA, [b]Institute of Materials Research and Engineering, 3 Research Link, Singapore 117602, [c]School of Materials Science and Engineering, Nanyang Technological University, 50 Nanyang Avenue, Singapore 639798, and [d]ACCE Research, Grand Vivier, F-38960 St Aupre, France

‡ Deceased.

Correspondence e-mail: hpweber@wanadoo.fr

Received 4 October 2007
Accepted 3 January 2008

Dedicated to the memory of our friend and colleague Richard K. McMullan

Three complete neutron diffraction datasets have been collected for deuterated malonic acid single crystals, $DOOC(CD_2)COOD$, above (153 K), just below (56 K) and further below (50 K) the low-temperature phase transition (T_c = 57 K). The structural details obtained for this transition, studied previously solely by spectroscopic and calorimetric techniques, clearly establish its first-order nature. At 153 K, the space group is $P\bar{1}$, $Z = 2$, $Z' = 1$. The molecules are packed as linear chains linked end-to-end by asymmetric hydrogen bonds so that the carboxyl groups form cyclic dimers. The deuterons in the carboxyl links are ordered. Neighboring chains are cross-linked through C—D···O hydrogen bonds. Upon cooling through the transition the cell doubles along the *a* axis. Molecules which are equivalent by symmetry above T_c become independent below T_c owing to conformational changes in alternate chains. At 50 K, the space group is $P\bar{1}$, $Z = 4$, $Z' = 2$. Thermal motion analysis, using for all three temperatures the same segmented rigid-body model, reveals a large torsional motion around the one COOD group associated with the conformational change. Refinements were carried out on all three datasets with an anharmonic structural model, including higher-order displacement tensors (Gram–Charlier expansion up to fourth order). Only atoms involved in torsional motion exhibit a significant anharmonic component which increases with temperature.

1. Introduction

Ubiquitous in nature, aliphatic dicarboxylic acids have been studied initially for their unusual intrinsic properties, but then, more recently, because of their suitability as model systems and building blocks in advanced materials. In the following we briefly highlight all these aspects.

The lower aliphatic dicarboxylic acids $HO_2C(CH_2)_nCO_2H$ (with $n = 0$ for oxalic acid, $n = 1$ for malonic acid, $n = 2$ for succinic acid *etc.*) are known for the bimodal distributions of their melting (Table 1) and boiling points, heats of combustion and solubilities, with all odd members of the series assuming lower values. This peculiar characteristic is explained by the observation that in all odd members, except oxalic acid, the carboxyl groups are rotated in opposite directions and are not co-planar – apparently a requirement for efficient molecular packing (MacGillavry *et al.*, 1948). Another peculiarity reported earlier is that all odd members undergo phase transitions just below their melting point (Dupré La Tour, 1932); this was interpreted by the former authors as a release from the internal strain that crystal packing imposes on the molecules at lower temperature.

Aliphatic dicarboxylic acids, particularly the short-membered ones, have long served as model systems to study

Table 1
Survey of aliphatic dicarboxylic acids $(CH_2)_nC_2H_2O_4$.

	Oxalic acid	Malonic acid	Succinic acid	Glutaric acid	Adipic acid	Pimelic acid	Suberic acid	Azelaic acid	Sebacic acid
Chemical formula	$C_2H_2O_4$	$(CH_2)C_2H_2O_4$	$(CH_2)_2C_2H_2O_4$	$(CH_2)_3C_2H_2O_4$	$(CH_2)_4C_2H_2O_4$	$(CH_2)_5C_2H_2O_4$	$(CH_2)_6C_2H_2O_4$	$(CH_2)_7C_2H_2O_4$	$(CH_2)_8C_2H_2O_4$
Melting point (K)	462–464	404–408	458–463	368–372	424–426	378–379	416–417	373–376	406
No. of known polymorphs	2	3	2	3	2	3	1	2	1
Phase γ									
Space group	–	$P\bar{1}$	–	$C2/c$	$P2_1/n$	$C2/c$	$P2_1/c$	–	–
Mol. symm.	–	None	–	Twofold	None	Twofold	$\bar{1}$	–	–
Temp. range (K)	–	13–56[a]	–	130	116–136	130	18–293	–	–
Structure	–	(*a*)	–	(*b*)	(*c*)	(*b*)	(*d*)	–	–
Twist angle†	–	**A** chain:	–	31.8 (1)	3.92 (1)	–	4.78	–	–
	–	76.86 (6)	–	–	10.39 (1)	–	–	–	–
	–	9.74 (8)	–	–	–	–	–	–	–
	–	**B** chain	–	–	–	–	–	–	–
	–	81.1 (1)	–	–	–	–	–	–	–
	–	6.52 (5)	–	–	–	–	–	–	–
Phase β									
Space group	$P2_1/c$	$P\bar{1}$	$P2_1/c$	$I2/a$	$P2_1/c$	$I2/a$	–	$C2/c$	$P2_1/c$
Mol. symm.	–	None	$\bar{1}$	Twofold	$\bar{1}$	Twofold	–	Twofold	$\bar{1}$
Temp. range (K)	12–298	57–352.2	77–410	293–347	136–293	293–348	–	180–353	180–293
Structure	(*e*) (*f*)	(*a*)	(*b*) (*g*)	(*h*) (*i*)	(*b*)	(*i*)	–	(*j*) (*k*)	(*l*) (*m*)
Twist angle†	–	88.84 (9)	11.01	–	10.66 (1)	30	–	62.2	2.2 (180 K)
	–	8.67 (7)	–	–	–	–	–	–	–
Phase α									
Space group	*Pcab*	*Pbcn*	Mcl	Mcl	–	$P2_1/c$	–	$P2_1/c$	–
Mol. symm.	–	Twofold	–	–	–	None	–	None	–
Temp. range (K)	12–298	352.2–??	410–??	347–??	–	$\sim$ 348	–	353	–
Structure	(*e*) (*f*)	(*n*)	(*o*) Unknown	(*o*) Unknown	–	(*p*), (*q*)	–	(*j*)	–
Twist angle†	–	46.6 (1)	–	–	–	18	–	16.11 (3)	–
	–	–	–	–	–	44	–	49.62 (4)	–

References: (*a*) this work, (*b*) Srinivasa Gopalan *et al.* (2000), (*c*) Srinivasa Gopalan *et al.* (1999), (*d*) Gao *et al.* (1994), (*e*) Derissen & Smith (1974), (*f*) Klooster *et al.* (2008), (*g*) Leviel *et al.* (1981), (*h*) Morrison & Robertson (1949), (*i*) MacGillavry *et al.* (1948), (*j*) Housty & Hospital (1967), (*k*) Bond *et al.* (2001*b*), (*l*) Housty & Hospital (1966*a*), (*m*) Bond *et al.* (2001*a*), (*n*) Delaplane *et al.* (1993), (*o*) Dupré La Tour (1932), (*p*) Housty & Hospital (1966*b*), (*q*) Kay & Katz (1958). † Twist angle of carboxyl plane with respect to carbon skeleton plane (°).

proton-transfer dynamics along the hydrogen bonds, using NMR (Meier *et al.*, 1982), inelastic neutron scattering (Kearley *et al.*, 1994) and other spectroscopic methods. Symmetric double-minimum potentials were shown to exist, even in hydrogen bonds that are not formally symmetric. Furthermore, the extensive polymorphism found in these small-chain molecules renders them eminently suitable as benchmarks in computer simulations to predict crystal structures (Beyer *et al.*, 2001; van Eijck, 2002). In particular, the conformational polymorphism prevailing amongst these dicarboxylic acids makes them particularly well suited to test new computational methods, as the structural differences between these polymorphs are simple and traceable to one or two variables. Finally, the structure of the new malonic acid polymorph presented here is amongst the comparatively rare cases (less than 10% of organic structures, Desiraju, 2007) with more than one independent molecule in the asymmetric unit. This is an additional reason why these solid acids are so well suited to test new crystal-structure prediction algorithms.

In the bottom-up design of new functional materials, the quasi-modular sequence of dicarboxylic acids such as oxalic acid, malonic acid, glutaric acids *etc.* takes a place of choice as polyvalent, supramolecular synthons (Leiserowitz, 1976; Rao *et al.*, 2004). For example, substituted malonic acids (Edwards *et al.*, 2002) and malonates (Ruiz-Pérez *et al.*, 2003; Delgado *et al.*, 2004) have recently been used in the design and synthesis of molecular magnets, where the innate flexibility of this dicarboxylic acid ligand permitted the formation of high-dimensional networks. The same chelating property of malonic acid has also been used to create metal malonate layers in a three-dimensional microporous network where these layers – with their metal sites accessible – were separated by pyridine-based pillars. Common to all these novel crystal engineering applications has been the beneficial use of the structural flexibility and the manifold types of intermolecular interactions inherent in these molecules, two qualities which also manifest themselves in the already mentioned polymorphism, details of which are still barely explored (Table 1).

In the specific case of malonic acid, evidence of polymorphism surfaced gradually, fed from a variety of observations. The first indication came from an ENDOR study carried out at 4.2 K (McCalley & Kwiram, 1970, 1993; Krzystek *et al.*, 1995). Compared with a previous, ambient-temperature deuteron NMR study (Derbyshire *et al.*, 1969), the number of

resonance lines was found to have doubled in the 4.2 K phase. Later, Raman and IR spectra measured over a range of temperatures confirmed the existence of this transition. To explain these spectral changes it was suggested that malonic acid doubles its unit cell while keeping its center of symmetry. Similar vibrational studies were carried out on the higher temperature β–α transition (Ganguly *et al.*, 1980; Villepin *et al.*, 1982; Bougeard *et al.*, 1988), prior to the elucidation of the structure of the α-phase crystal (Delaplane *et al.*, 1993). In parallel, calorimetric measurements over the temperature range 13–371 K suggested (Fukai *et al.*, 1991) that the two phase transitions, γ–β as well as β–α, are first-order, as they exhibit quite sharp maxima of the specific heat capacity. The same authors observed that:

(i) at the transition γ and β co-existed over a 2 K temperature range, and

(ii) that the volume ratio of the γ and β domains depended on the thermal history of the sample.

It thus seemed as if the displacive transition was martensitic in character.

At ambient conditions, the only crystal structure known for malonic acid for almost half a century was that determined from photographic data (Goedkoop & MacGillavry, 1957). Recently a more precise, low-temperature (130–145 K) charge-density study of the lower carboxylic acids (n = 2–5), including malonic acid (Srinivasa Gopalan *et al.*, 2000), confirmed the essential correctness of the β phase. At ambient temperature and all the way down to the β–γ transition, the crystal structure of malonic acid is triclinic (Z = 2), while all other members of the higher carboxylic acid series assume monoclinic symmetry at ambient temperature (Table 1). The molecules are packed as infinite, all-*trans* zigzag chains linked head-to-tail so that the carboxyl groups form cyclic dimers. In contrast to the higher carboxylic acids, where the two carboxyl groups of each molecule are related by symmetry (either an inversion centre or twofold axis), the carboxyl rings in malonic acid are crystallographically non-equivalent and nearly orthogonal to each other. Above the β—α transition (T_c = 358 K; Jagannathan & Rao, 1987) the structure displays orthorhombic symmetry, with Z = 4 (Delaplane *et al.*, 1993). The molecules still form zigzag chains, but the carboxyl groups have become crystallographically equivalent and are related by a twofold symmetry axis.

Initially, the present study was undertaken to provide accurate positional and displacement parameters for a charge-density study. When in the course of this work a phase transition was observed unexpectedly at 56 K (and later confirmed by NMR measurements, Krzystek *et al.*, 1995), focus shifted to a description of the structural phase transition. Our study is only the third published neutron diffraction study of a member of this important class of compounds,[1] the other being succinic acid (Leviel *et al.*, 1981) and suberic acid (Gao *et al.*, 1994). Although the NMR study already published in the meantime reveals some structural aspects of the low-temperature phase, the full description of molecular conformation, packing and other important structural details had to await the results of the present study.

2. Experimental

Malonic acid, $C_3H_4O_4$ (Aldrich Chemical), was repeatedly recrystallized from a D_2O solution to yield crystals of isotopic purity, 92% $C_3D_4O_4$, as determined from the structure refinements. The crystal used for diffraction measurements was coated with halocarbon grease under nitrogen gas and sealed in an aluminium canister under helium gas. The diffraction measurements were performed in 1986 and 1987 during two different reactor cycles at the Brookhaven High Flux Beam Reactor on four-circle diffractometers at ports H6M and H6S. Monochromated neutron beams were obtained from Be (002) planes in reflection and Ge (220) planes in transmission geometries; the respective wavelengths of 1.0411 (1) and 1.1588 (1) Å were calibrated against a KBr crystal (a_0 = 6.6000 Å at 295 K). The diffraction data were recorded first at nominal temperatures of 123 and 20 K and then, during a later period, at 56 K. The sample crystal was held within $\pm 0.1^\circ$ of the preset temperature using helium cryostats (DISPLEX Model CS-202, Air Products & Chemical, Inc.). Reflection scan widths and intensities were monitored for changes in crystal integrity while cooling to the target temperatures. The $\bar{1}01$ reflection showed a sharp and reversible intensity change, which was attributed to a phase transition occurring between 123 and 20 K on the sensor scale. Scans in 2θ along a^*, b^* and c^* revealed halving in a^* and no other marked changes in the lattice below the transition. Integrated intensities of superlattice reflections $\bar{3}25$ and $\bar{1}24$ were measured at 1° increments through the phase transformation in attempts to fix the transition point on the sensor scale. The transition temperature, T_c, of 27 K determined by the sensor was judged to be unusually low for a structural phase change. Subsequently, in the second diffraction study, the value of T_c was determined by the same procedure to be 57 K against the sensor checked by an independent calibration (Fig. 1S, supplementary material[2]). The revised value is within the ranges determined for deuterated malonic acid by NMR (Krzystek *et al.*, 1995) and for protonated malonic acid by neutron diffraction (Delaplane *et al.*, 1993). The nominal measurement temperatures, 20 and 123 K, were assumed to be in error and were corrected by $+30^\circ$ with reference to T_c = 57 K as a fixed point. This T_c is slightly lower than the value observed calorimetrically for fully deuterated malonic acid (60 K; Fukai *et al.*, 1991), but much higher than the corresponding value for the hydrogenated form (47.3 K). This agrees well with our refinement results, where deuterium is shown to have exchanged to 91.7 (8)% for hydrogen.

Absorption corrections (de Meulenaer & Tompa, 1965; Templeton & Templeton, 1973) were applied using the

[1] With an additional neutron study underway on anhydrous oxalic acid (Klooster *et al.*, 2008).

[2] Supplementary data for this paper are available from the IUCr electronic archives (Reference: BK5069). Services for accessing these data are described at the back of the journal.

Table 2
Experimental details.

	50 K	56 K	153 K
Crystal data			
Chemical formula	$C_3D_4O_4$	$C_3D_4O_4$	$C_3D_4O_4$
M_r	69.853	69.853	69.853
Cell setting, space group	Triclinic, $P\bar{1}$	Triclinic, $P\bar{1}$	Triclinic, $P\bar{1}$
Temperature (K)	50 (1)	56 (1)	153 (1)
a, b, c (Å)	10.663 (4), 5.142 (2), 11.234 (2)	10.675 (1), 5.152 (1), 11.238 (1)	5.333 (2), 5.158 (2), 11.250 (2)
α, β, γ (°)	103.39 (3), 136.81 (2), 85.19 (3)	103.35 (1), 136.68 (1), 85.07 (1)	103.33 (3), 136.40 (2), 84.76 (3)
V (Å^3)	406.8 (3)	409.45 (13)	206.34 (15)
Z	4	4	2
Z'	2	2	1
D_x (Mg m^{-3})	1.758	1.747	1.733
Radiation type	Neutron	Neutron	Neutron
μ (mm^{-1})	0.02	0.02	0.02
Crystal form, color	Prism, colorless	Prism, colorless	Prism, colorless
Crystal size (mm)	2.0 × 2.4 × 3.0	2.0 × 2.4 × 3.0	2.0 × 2.4 × 3.0
Data collection			
Diffractometer	Four-circle diffractometer H6S	Four-circle diffractometer H6M	Four-circle diffractometer H6S
Data collection method	ω–2θ scans	ω–2θ scans	ω–2θ scans
Monochromator	Ge (220)	Be (002)	Ge (220)
Scan range = $a + b \sin\alpha$			
a, b (°) ($5 < 2\theta < 55°$)	3.0, 0.0	3.0, 0.0	3.0, 0.0
a, b (°) ($55 < 2\theta < 108°$)	1.45, 3.01	1.44, 3.44	1.45, 3.01
Points per scan	65	65	65
$(\sin\theta/\lambda)_{max}$ (Å^{-1})	0.70	0.79	0.70
Absorption correction	Analytical	Analytical	Analytical
T_{min}	0.95	0.95	0.95
T_{max}	0.97	0.97	0.97
No. of measured, independent and observed reflections	2653, 2307, 2307	4641, 3203. 3203	1345, 1177, 1177
Criterion for observed reflections	$I > 2\sigma(I)$	$I > 2\sigma(I)$	$I > 2\sigma(I)$
R_{int}	0.019	0.022	0.011
θ_{max} (°)	54.2	55.3	54.2
Refinement			
Refinement on	F^2	F^2	F^2
$R(F^2)$, $wR(F^2)$, S†	0.038, 0.052, 1.53	0.035, 0.049, 1.02	0.031, 0.038, 1.01
No. of reflections	2300	3205	1177
No. of parameters	208	208	105
Weighting scheme	$w = 1/[\sigma^2(F_o^2) + (0.02F_o^2)^2 + 0.05]$	$w = 1/[\sigma^2(F_o^2) + (0.02F_o^2)^2]$	$w = 1/[\sigma^2(F_o^2) + (0.02F_o^2)^2 + 514]$
$(\Delta/\sigma)_{max}$	< 0.0001	< 0.0001	< 0.0001
$\Delta\rho_{max}$, $\Delta\rho_{min}$ (e Å^{-3})	0.27, −0.40	0.45, −0.50	0.53, −0.60
Extinction method	Becker & Coppens	Becker & Coppens	Becker & Coppens
Extinction coefficient	0.102 (2)	0.103 (3)	0.125 (3)

Computer programs used: *ABSOR* (adopted from de Meulenaer & Tompa, 1965; Templeton & Templeton, 1973), *NOOT* (Craven *et al.*, 1991), *UPALS* (Lundgren, 1982), *THMA*13 (Schomaker & Trueblood, 1998), *DIAMOND* (Brandenburg, 2007). † $R(F^2) = \Sigma\Delta/\Sigma F_o^2$; $wR(F^2) = [\Sigma w\Delta^2/\Sigma(wF_o^2)^2]^{-1}$; $S = [\Sigma w\Delta^2 n - p]^{1/2}$, where $\Delta = |F_o^2 - F_c^2|$, and n and p are the numbers of observations and parameters, respectively.

isotopic D/H composition of 8%H from initial structure refinements and assuming the mass absorption coefficients of hydrogen to be 26.41 and 24.75 cm^2 g^{-1} at wavelengths of 1.1588 and 1.0411 Å (Koetzle & McMullan, 1980). The calculated transmission factors T_f varied between 0.95 and 0.97. The averages of symmetry-related F_o^2 ($I_0 T_f^{-1} \sin 2\theta$) values for ($0 \pm k \pm l$) reflections gave the agreement factors shown in Table 2.

3. Structure determinations

Initial carbon and oxygen positions of the β-phase structure were taken from the X-ray analysis of Goedkoop & MacGillavry (1957) and were adjusted by Fourier methods against the 153 K neutron data. The hydrogenic atoms were all located as positive peaks in a difference map, indicating that deuteration was uniform and largely complete in the crystal. In the γ phase[3] a similar centrosymmetric arrangement of molecules was inferred from the obvious relationship in the lattices of the two phases (Table 2). The two independent molecules were determined by choosing between the alternate inversion centers along the ***a*** direction of the subcell; the centers that relate hydrogen-bonded carboxyl groups were retained, and this choice was verified by the structure analysis. Refinements were carried out with the full-matrix least-squares programs of Lundgren (1982) and Craven *et al.* (1991). The residuals $\Sigma w|F_o^2 - F_c^2|^2$ were minimized with weights $w = [\sigma_c^2(F_o^2) +$

[3] The notation for the three polymorphs introduced by the previous authors (MacGillavry *et al.*, 1948; Krzystek *et al.*, 1995) was kept, even though it is contrary to custom (see Bernstein, 2002, for a discussion on this point).

$(0.02F_o^2)^2$ + const.]$^{-1}$, summing over the independent observations with $F_o^2 \geq 0.0$. Coherent neutron-scattering lengths (fm) for H (−3.7409), D (6.674), C (6.6484) and O (5.803) were taken from the tabulation of Koester (1977). The variable parameters were the atomic coordinates and anisotropic displacement parameters [up to fourth order in the Gram–Charlier expansion; Johnson & Levy, 1974, equation 5.2.3(9), but retaining eventually only the significant third-order terms], scattering lengths at deuterium/hydrogen sites, one scale factor and the isotropic secondary extinction parameter for a type I crystal (Becker & Coppens, 1974) with a Lorentzian distribution of mosaicity. The data were extensively affected by extinction with 318, 348, 180 (50, 56, 153 K) reflections having applied corrections greater than 5%. Reflections in each dataset with corrections (xF_o^2) greater than 1.5 (7 at 50 K, 1 at 56 K and 7 at 153 K) were omitted from the final refinement cycles. The refinements converged with all parameter changes, $\Delta p_I/\sigma(p_I)$, < 0.001. Table 2 summarizes the details of the refinements. In the final $\Delta\rho$ maps for the 50, 56 and 153 K data, the largest residual errors were ∼ 1.9, 1.5 and 1.5% of the maximum peak height at carbon in the corresponding ρ_0 maps.

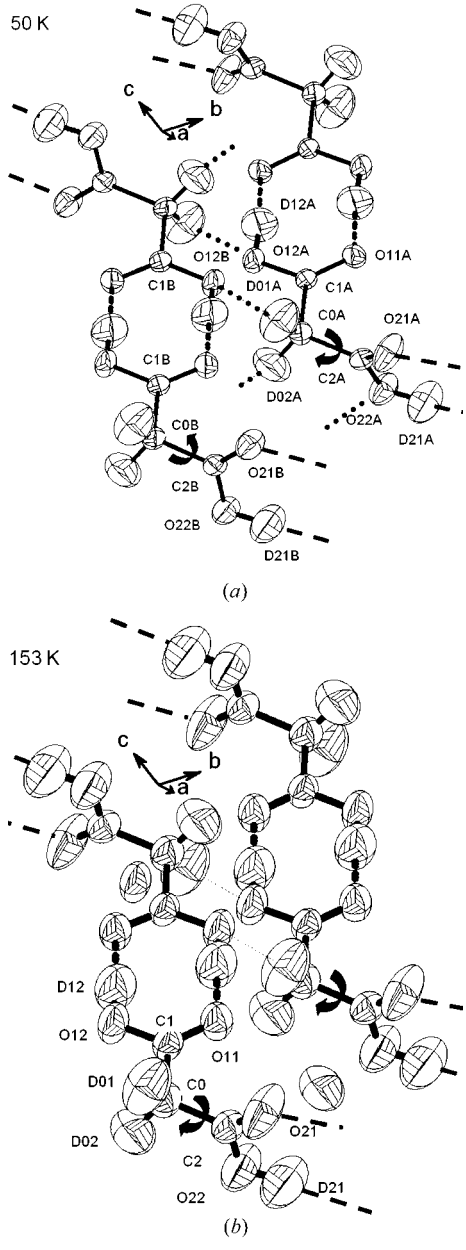

Figure 1
Perspective views of malonic acid molecules, hydrogen-bonded across inversion centers and in the same mutual orientation as observed in the crystal structures, with atomic notation as used in the text. Intermolecular hydrogen bonds are sketched as dashed (O—D—O) and dotted (C—D···O) lines. Bent arrows indicate a sense of torsional motion around the C0—C2 bond. The ellipsoidal surfaces enclose 99.9% probability (Johnson, 1976). (*a*) γ phase at 50 K; (*b*) β phase at 153 K.

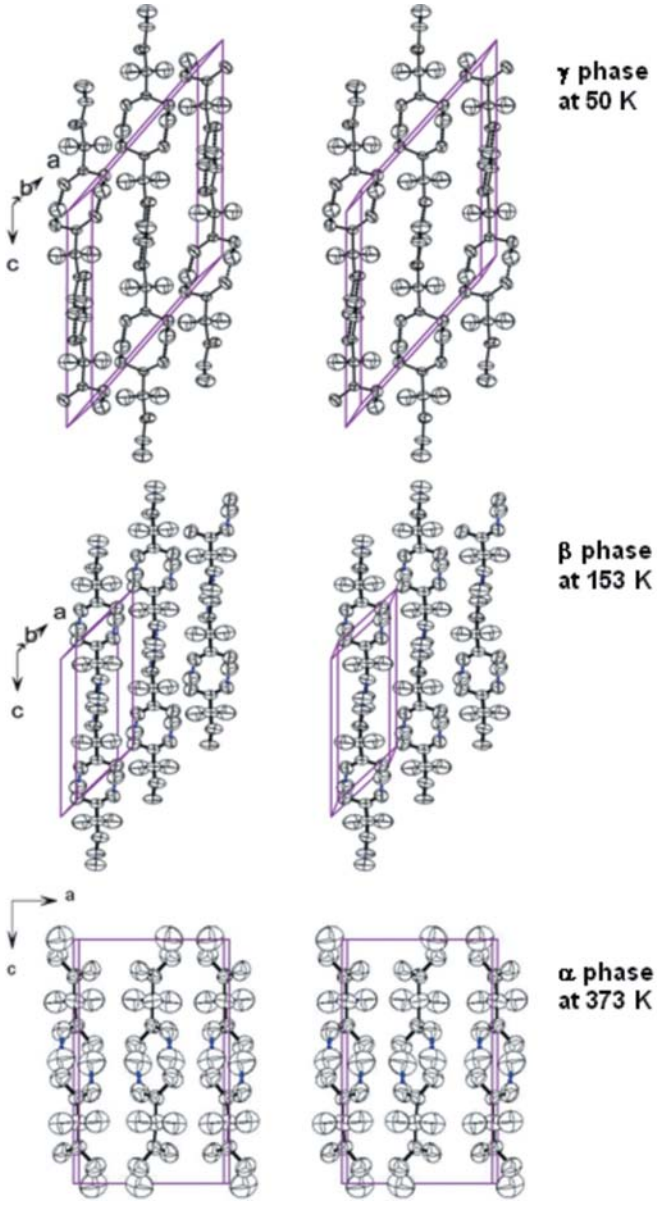

Figure 2
Stereo diagrams of the α (Delaplane *et al.*, 1993), β and γ phase (this work) neutron structures viewed approximately down **b***. The ellipsoidal surfaces enclose 99% probability for the β and γ phases, and 50% for the α phase.

Table 3
Short non-bonded interactions for all three phases of malonic acid.

Bond lengths (Å) first line, bond angles (°) second line. Short interactions are in terms of van der Waals distances (H···O 2.6, C···O 3.2 Å).

	50 K	56 K	153 K	373 K[(a)]
(*a*) Attractive				
O—D···O type				
Intermolecular				
O11*A*···D12*B*	1.688 (1)	1.687 (1)	1.681 (1)	1.648 (8)
O11*A*···D12*B*—O12*B*	172.77 (9)	173.22 (8)	174.50 (9)	176.3 (6)
O11*B*···D12*A*	1.663 (1)	1.6652 (8)		
O11*B*···D12*A*—O12*A*	175.79 (9)	175.57 (8)		
O21*A*···D21*B*	1.702 (1)	1.696 (1)	1.690 (1)	
O21*A*···D21*B*—O22*B*	175.62 (9)	176.27 (8)	177.11 (9)	
O21*B*···D21*A*	1.684 (1)	1.684 (1)		
O21*B*···D21*A*—O22*A*	177.03 (9)	177.14 (8)		
C—D···O type				
Intermolecular				
D01*A*···O12*B*^{i}	2.450 (2)	2.460 (1)	2.499 (4)	2.593 (9)
C0*A*—D01*A*···O12*B*	165.76 (9)	165.41 (7)	163.62 (9)	138.3 (8)
D01*B*···O12*A*^{i}	2.533 (2)	2.528 (1)		
C0*B*—D01*B*···O12*A*	163.9 (1)	163.69 (7)		
D02*A*···O22*B*^{ii}	2.495 (2)	2.519 (2)	2.600 (4)	
C0*A*—D02*A*···O22*B*	147.46 (9)	147.84 (8)	149.9 (1)	
D02*B*···O22*A*^{ii}	2.577 (2)	2.593 (1)		
C0*B*—D02*B*···O22*A*	154.8 (1)	153.39 (7)		
Intramolecular				
D01*A*···O12*A*	2.674 (2)	2.676 (2)	2.648 (4)	2.414 (9)
C0*A*—D01*A*···O12*A*	60.7 (1)	60.80 (8)	61.2 (1)	73.2 (7)
D01*B*···O12*B*	2.644 (2)	2.651 (2)		
C0*B*—D01*B*···O12*B*	62.32 (9)	62.08 (7)		
D01*A*···O21*A*	2.555 (2)	2.563 (2)	2.595 (3)	
C0*A*—D01*A*···O21*A*	69.1 (1)	68.74 (5)	67.11 (7)	
D01*B*···O21*B*	2.633 (2)	2.624 (1)		
C0*B*—D01*B*···O12*B*	65.78 (6)	66.05 (5)		
D02*A*···O22*A*	2.558 (2)	2.544 (1)	2.493 (4)	
C0*A*—D02*A*···O22*A*	67.28 (6)	67.92 (5)	69.92 (8)	
D02*B*···O22*B*	2.477 (2)	2.481 (1)		
C0*B*—D02*B*···O12*B*	71.16 (6)	71.08 (5)		
D02*A*···O12*A*	2.528 (2)	2.533 (2)	2.522 (3)	
C0*A*—D02*A*···O12*A*	67.76 (6)	67.58 (5)	67.20 (7)	
D02*B*···O12*B*	2.555 (2)	2.555 (2)		
C0*B*—D02*B*···O12*B*	66.57 (6)	66.64 (5)		
(*b*) Repulsive				
Intramolecular				
C0*A*···O11*A*	2.405 (2)	2.407 (1)	2.403 (1)	2.402 (9)
C0*B*···O11*B*	2.405 (2)	2.407 (1)		
C0*A*···O12*A*	2.344 (2)	2.345 (1)	2.328 (4)	2.343 (9)
C0*B*···O12*B*	2.345 (2)	2.347 (1)		
C0*A*···O21*A*	2.394 (2)	2.394 (1)	2.392 (4)	
C0*B*···O21*B*	2.401 (2)	2.398 (1)		
C0*A*···O22*A*	2.344 (2)	2.361 (1)	2.353 (3)	
C0*B*···O22*B*	2.362 (2)	2.365 (1)		

References: (*a*) Delaplane *et al.* (1993). Symmetry codes: (i) $1-x, -y, 1-z$; (ii) $-x, -y, -z$.

The final nuclear positional and anisotropic displacement parameters are listed in Table 1S of the supplementary material. The molecular conformation in the unit cells, together with atomic notation and displacement ellipsoids, are illustrated in Figs. 1 and 2. Bond lengths and angles are given in Tables 2S and 3S. Additional tables and figures are available as supplementary material.

4. Discussion

In the ensuing discussion of our results, we often refer to observations made in structural studies of other aliphatic dicarboxylic acids (Table 1). This systematic comparison permitted us to uncover and ascertain trends, which if based solely on results from malonic acid might not have attained the desired level of certainty.

4.1. Structures at 50, 56 and 153 K

In both the β and γ phases the H atoms are ordered and positioned asymmetrically. In the lowest temperature γ phase, the malonic acid molecules [DOOC(CD_2)COOD] form linear chains along [001], with the carboxyl groups providing the cyclic dimer links (Fig. 2). The O—H···O intermolecular hydrogen bonds linking the dimers are the strongest intermolecular bonds in the dicarboxylic acids (Table 3) and they are one of the structure-determining factors. The chains are stacked along [100], with the molecules alternating their conformation along this direction. The stacks themselves are held together by intermolecular hydrogen bonds between the methylene groups and the O atoms from neighboring molecules. While initially it was thought as unusual for hydrogen from methylene groups to form hydrogen bonds, this bond type has in the meantime become widely accepted, thanks to surveys of hydrogen-bonded structures determined by neutron diffraction (Taylor & Kennard, 1982; Desiraju, 1996). Such bonds never violated any physical law; they simply lay outside the then customary definition of the hydrogen bond. In the solid state these weak hydrogen bonds are most commonly observed between molecules, but there are also occurrences where the hydrogen of methylene acts as an intramolecular bridge, as in γ-aminobutyric acid (Weber *et al.*, 1983). In the charge-density study of this compound (Craven & Weber, 1983) the bridging methylene hydrogen was found to be positively charged, which possibly explains the ease with which D substituted for the methylene H atoms during isotopic substitution in our malonic acid sample.

In passing we should not fail to point out that we can safely discard the hypothesis whereby the high-temperature β-structure of malonic acid is a disordered, average structure and results from the superposition of the positions of molecules *A* and *B*. Averaging the coordinates of molecules *A* and *B* of the lowest-temperature (50 K) γ phase yields the higher-temperature (153 K) structure only for the carbon skeleton; it does not reproduce the positions of the carboxylate end groups.

4.2. Thermal motion below and above the β–γ phase transition

Modeling the thermal motion of molecules in a crystalline compound in terms of the nuclear anisotropic displacement parameters (ADP) of the individual molecules has its limitations. Foremost, the ADPs are the sums of mean-square displacement over all vibrational modes; we cannot reconstruct the contributions of the individual modes (external and internal). However, we can, under special circumstances,

Table 4
Rigid-body thermal vibrations.

Tensor components for translation (Å^2 × 10^4), libration (deg^2) and screw motion (radian × Å × 10^4) are referred to the inertial frame, with the center of mass as the origin.

	50 K		56 K		153 K
Molecule	*A*	*B*	*A*	*B*	
T11	40 (4)	40 (5)	47 (4)	46 (3)	91 (7)
T22	61 (5)	60 (9)	94 (5)	82 (5)	127 (8)
T33	50 (5)	58 (8)	65 (5)	81 (5)	118 (7)
T12	7 (3)	1 (1)	−2 (2)	−19 (7)	−9 (7)
T13	−2 (1)	9 (7)	−2 (2)	10 (3)	−6 (7)
T23	2 (1)	7 (2)	2 (3)	−11 (4)	−1 (7)
L11	11 (1)	10 (1)	18 (3)	11 (2)	60 (2)
L22	2 (1)	2 (1)	3.2 (5)	3.2 (2)	12 (1)
L33	0.8 (2)	1.2 (3)	0.2 (4)	1.8 (1)	5 (2)
L12	0.3 (2)	0.6 (2)	1.2 (7)	1.2 (1)	9 (2)
L13	4 (1)	−0.2 (1)	1.6 (6)	1.1 (2)	3 (2)
L23	0.9 (2)	0.9 (8)	0.14 (5)	−0.4 (6)	−4 (1)
S11	0 (1)	−2 (1)	−3 (1)	−6 (1)	−5 (3)
S12	5 (1)	−3 (1)	19 (3)	1 (1)	−1 (22)
S13	−9 (2)	9 (2)	−13 (2)	−1 (1)	−3 (21)
S21	−3 (1)	−0 (12)	−5 (1)	−1 (1)	−1 (15)
S22	−3 (1)	4 (1)	−2 (1)	11 (2)	7 (28)
S23	3 (1)	−3 (1)	1 (1)	−3 (1)	4 (14)
S31	0 (1)	−2 (1)	1 (1)	−1 (1)	5 (22)
S32	1 (1)	−0 (1)	2 (1)	2 (1)	3 (23)
S33	3	−3	5	−5	−2
$\langle\varphi^2\rangle$ C0−C (deg^2)	26 (3)	15 (4)	42 (8)	4 (4)	64 (5)
wR	0.07	0.10	0.06	0.08	0.06
GoF	1.52	1.84	1.72	1.25	2.63

separate out a contribution of a dominant type (see *e.g.* Weber *et al.*, 1991). The interpretation of the ADPs in molecular crystals is based on the identification of rigid groups of atoms and on the description of their collective thermal motion. The physical basis of this concept is that the intramolecular binding forces are much stronger than the intermolecular ones and that the low-frequency external modes contribute disproportionately more to the ADPs than the high-frequency modes. This and the fact that the contribution of the internal modes to the ADPs is not only small, but nearly temperature-independent, finally permits modeling the thermal motion of the molecule.

We have analyzed the ADPs of malonic acid in terms of just such a mechanistic rigid-body motion (RBM) of the molecular backbone, adding, as needed, additional libration motion of molecular fragments around selected bonds as axes. The RBM explicitly introduces the correlation between the atoms of the vibrating molecule, a quantity the experiment (Bragg diffraction) cannot provide. The results of such an analysis (Schomaker & Trueblood, 1998; Dunitz & White, 1973; Bürgi, 2000) may be visualized in terms of a superposition of independent simple motions of the rigid body: three translations and three librations about a set of non-intersecting axes parallel to the principal axes of libration. In the absence of inversion symmetry (which is the case for γ- and β-malonic acid) these six degrees of freedom mix into six screw motions. Table 4 lists the results obtained for γ- and β-malonic acid at the three temperatures of interest.

In a first step, the complete molecule was included in the analysis. The residual $\Sigma w\Delta_R^2$ was minimized. In this expression $\Delta k = [(U^{ij})_{\rm obs} - (U^{ij})_{\rm calc}]_k$, where $(U^{ij})_{\rm obs}$ is the neutron value for an ADP for the kth atom, referred to the Cartesian crystal axial system a,b,c^*, and $(U^{ij})_{\rm calc}$ is the corresponding value calculated for the assumed thermal motion. The weights $w_k = \sigma^{-2}(U_k)$ are obtained from the mean variances in U^{ij} for the kth atom. The fit was poor, as judged by $wR = [\Sigma w\Delta^2/\Sigma w(U^{ij})_{\rm obs}^2]^{1/2}$, > 0.17 for all three temperatures. A far better fit was obtained when all the deuterons were omitted. However, without the deuterons and omitting the carbonyl O atoms, the remaining nuclei lie close to two parallel, straight lines. Also, unfortunately in this case, as Johnson (1980) pointed out, the least-squares normal equation matrix turns almost singular. This is why we then retained the parameters for the methylene H atoms as observations, but assigned to them m.s. (mean-square) displacements corrected for the internal vibrations of the CD_2. To this end, we assumed that the molecular rigid body or lattice vibrations were not correlated with the intramolecular non-rigid (internal) vibrations so that the corresponding m.s. displacements are simply additive (Higgs, 1953). We subtracted from the experimental m.s. displacements 0.0032 Å^2 for the C—D stretching vibrations, 0.0137 Å^2 for the C—D_2 in-plane vibrations and 0.0122 Å^2 for the C—D_2 out-of-plane vibrations. These values were averages for the 11 methylene groups of the hexanoate anion in deuterated piperazinium hexanoate (Luo *et al.*, 1996). The rigid-body fit obtained with inclusion of all deuterons was then much improved, with wR = 0.123 (molecule *A* at 50 K), 0.127 (molecule *B* at 50 K) and 0.131 (at 153 K). We then resorted to a more elaborate model for the molecular motion. Rather than letting ourselves be guided purely by chemical intuition – which suggested that rotational motion takes place around one or both of the central C2—C0—C1 bonds – we computed first the mean-square vibrational amplitudes of intramolecular atom pairs *A* and *B* in the direction of the interatomic vector *A*···*B*. For any pair of atoms of comparable mass these amplitudes should be about the same if the molecule they are part of is rigid.[4] In other words, the difference $\Delta = \langle u_A^2\rangle - \langle u_B^2\rangle$ should be non-zero only if atoms *A* and *B* are not rigidly connected. This condition is necessary but not sufficient for the molecule to behave as a rigid body. Inspection of the values of Δ for all pairs of atoms of equal mass in the two molecules of the γ phase at 50 K reveal several large differences (Table 4S of the supplementary material). First, the O atoms from opposing carboxylic groups exhibited large differences [*e.g.* Δ = 0.0065 (7) Å^2 for O21···O11 in molecule *A*], with consistently larger values for molecule *A* than for molecule *B*. It was thus evident that:

(i) neither molecule *A* nor *B* behaved as a rigid body, and

(ii) that molecule *A* exhibited more internal motion than molecule *B*.

[4] This observation is attributed to K. N. Trueblood (see Johnson, 1980).

Secondly, while Δ O22$\cdots$C1 = 0.0081 (8) (molecule *A*) and 0.0034 (5) Å^2 (molecule *B*), the corresponding values amounted to only 0.0008 (4) and 0.0005 (4) Å^2, respectively, for the chemically equivalent non-bonded interaction O12$\cdots$C2 (see Fig. 1*a*). From this we inferred that the C2—C0 axis was far more likely to act as an additional rotation axis than C1—C0. Still, in the following both models were tested. In the low-temperature γ phase the C2—C0 axis was found to be the preferred axis of rotation for molecule *A*, while for molecule *B* intramolecular libration was barely significant; molecule *B* seemed to behave in a quasi-rigid fashion. In the higher-temperature β-phase, large librational motion again revealed itself around the C2—C0 connecting bond. This model (Table 4) gave satisfactory agreement for the displacement parameters of both backbone atoms and terminal groups; the most significant residuals being 4.1σ for ΔU^{33} of O11 and -5σ for ΔU^{11} of C1. As noted in previous studies the fit was again better for the higher-temperature data. The torsional motion of the O21—C2—O22—D21 group is large for such a low temperature. If extrapolated linearly to the temperature of the β–α transition (352 K) it amounts to 122 deg^2.

The dissimilarity in torsional amplitude between *A* and *B* molecules can be explained. Both ends of the *B* molecule are tied down *via* weak hydrogen bonds to methylene D atoms of the neighboring *A* molecule (see Fig. 2); although the reverse is also true, the C—D$\cdots$O hydrogen bonds are noticeably weaker for the *B* molecule (Table 3). These contacts already exist in the β phase, but with the lowering of the temperature and the transition to the γ structure, their lengths decrease by 0.05–0.1 Å. In both β and γ phases the contact angles are already favorably close to regular hydrogen-bond values (compared with the α-phase where the angle is 138°). A similar accommodation takes place at the β–γ phase transition in adipic acid (Srinivasa Gopalan *et al.*, 1999).

Another interesting observation, which attests to the essential correctness of our model, is that the minimum moment of inertia of the molecules and the axis of maximum libration, L_3, enclosed in all cases an angle of at most 6°. Furthermore, the translational displacement tensor is very anisotropic, with the direction of largest translational motion, T_2, for all molecules and at all temperatures almost parallel to the *c* axis. This reflects the fact that the closest intermolecular repulsive contacts are between molecules in the chain stacks, *i.e.* along **a***.

The large librational motion is unusual for such a low temperature and may lead to a deviation of the probability density functions (p.d.f.s) describing thermal motion from Gaussian shape. So, in the refinement of the ADPs, we modified these to include anharmonic terms. This was done by including higher-order terms (up to fourth-order), using the Gram–Charlier expression given by Johnson & Levy (1974), see equation 5.2.3(9). At first, these higher-order displacement tensors were included for all O and D atoms; then, in later refinements, only those higher-order terms were retained which had proven to be significant at the greater than 3σ level in the former refinements. It turned out that such significant anharmonicity was noticeable only in the 153 K data, and solely for the O21 atom. The same atom at lower temperature was again the only one which exhibited a few third-order terms, albeit at a level of significance barely attaining 3σ. The probability density for both total and solely third-order contribution is shown for this atom in Fig. 3. The skewness of the thermal motion is due to the environment of O21 and does not seem related to the phase transition. The displacement ellipsoid of the carbonyl oxygen does not show any significant deviation from harmonicity.

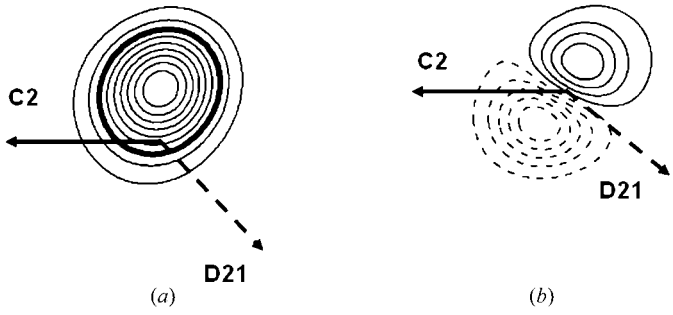

Figure 3
Section through the p.d.f.s of O21 at 153 K in the plane of the carboxylic group. The section measures 1 × 1 Å. (*a*) Total p.d.f. up to third order in the Gram–Charlier expansion. The contour level with 50% probability is drawn with a heavier line; the contour interval is 440. Arrows point to atoms to which O21 is bonded. (*b*) The p.d.f. with only third-order terms (skewness) of the Gram–Charlier expansion plotted; the contour interval is 130.

4.3. Conformational changes and the phase transition

In general, the hydrocarbon backbone of the aliphatic dicarboxylic acids – like the alkanes from which they are derived – crystallize in an all-*trans* planar conformation, while in solutions the conformation of the hydrocarbon backbone depends on the nature of the solvent (Fukushima *et al.*, 1986). For even-numbered acids the carboxylic tail groups are coplanar, or nearly so, with the carbon backbone, while the carboxyl plane of the odd-membered ones is considerably twisted away from the carbon-skeleton plane (see Table 1). The same pattern is observed for their salts. This effect is likely to arise from the demands efficient packing puts on the geometry of the carboxylic dimerization. This odd–even packing effect is already observed in two dimensions, where in thin films of self-assembled saturated carboxylic acids deposited from solutions onto oriented pyrolytic graphite (Hibino *et al.*, 1998; Tao *et al.*, 2006) the orientation of the carboxylic groups depends on the length of the alkyl chains.

In *ab initio* calculations on malonic acid (Merchán *et al.*, 1984; Tarakeshwar & Manogaran, 1996) the global conformation of the monomer found to be stable was always the one with the two carboxyl groups orthogonal to each other, a conformation similar to that observed for the monomers in the β and γ phases. Planar conformers with and without an intramolecular hydrogen bond between the carboxyl groups of the same molecule were shown to have a higher energy, this

being attributed to steric hindrance between the two groups. However, more recent (Maçôas *et al.*, 2000) and higher-level computations (MP2 approximation as well as density functional theory) of relative energies and vibrational spectra revealed a basis-set dependence of the stability ranking of the three lowest-energy conformers [(I): nearly planar, with intramolecular hydrogen bond; (II): carboxylic groups nearly orthogonal, with one carboxylic group coplanar with the C-atom backbone, corresponding to the conformation in the α structure; (III): with both carboxylic groups out of the plane containing the skeletal carbon, corresponding to the β structure conformation], thereby emphasizing the small difference in energy between the conformers (< 5 kJ mol^{-1}). Finally, IR spectra collected by the same authors on malonic acid monomers embedded in an argon matrix provided an experimental confirmation of their theoretical calculations: All three conformers were observed, with a population distribution favoring the fully extended, planar conformers (77%). This experimental, spectroscopic evidence supports the conjecture originally advanced by MacGillavry *et al.* (1948), whereby it is the crystal packing forces – generally the environment – which *in fine* impose on the conformers a deviation from planarity. At the time the conjecture was advanced, however, few crystal structures of aliphatic dicarboxylic acids had been determined. In the half century elapsed since, this structural gap has been closed. From the survey of the crystal structures of the lower dicarboxylic acids (Table 1) it is now evident that with increasing chain length the terminal carboxylic groups play an increasingly minor role in the crystal packing of the chains. With increasing chain length, the fatty acid character takes over, the lateral interactions between the alkyl moiety of the molecules become the dominant factor in the stability of their crystal structure. This is reflected in a reduced polymorphism and steadily decreasing melting points (Table 1). The lower dicarboxylic acids, up to azelaic acid, are too short-chained to exhibit fatty acid character, and their crystal structures are atypical.

Information obtained from elastic scattering experiments generally yields few clues as to the driving force in a phase transition. Nevertheless, unusual changes in conformation or unexpectedly large torsional motions, recorded as a function of temperature, often hint at the nature of the transition mechanism. In the specific case of malonic acid, an analysis of its conformational changes (Table 1) taking place in the molecules during the transition revealed the following features in order of decreasing significance:

(i) the C2 carboxylate tails twist alternately in a clockwise (molecule *A*) and an anticlockwise (molecule *B*) direction by more than 10°, and

(ii) the opposite carboxylate end exhibits the same behavior, although on a much reduced scale ($\sim 2°$).

This is consistent with the rigid-body motion analysis where internal rotation around the C0—C2 bond was found at 50 and 56 K to be much more pronounced than for the C0—C1 axis – as if it were a harbinger of an impeding phase transition.

There are few accurate crystal structures presently available for the lower odd-membered aliphatic dicarboxylic acids, and several phase transitions for which the only available data are more than seven decades old and unconfirmed since. Yet, it is tempting to outline a scenario for their polymorphism. At the lowest temperature heat input is absorbed first by the torsional motion of the carboxylic tail-ends and the C—D···O attractive interactions, lessening their twist away from the hydrocarbon backbone. This conformational change costs little energy and thus a first phase transition already takes place at very low temperature. Somewhat straightened out, the alkyl chains can then, upon a further, larger increase in temperature, slip past each other, along the direction of their largest translational vibration. This structural change is more costly and the second phase transition takes place at a far higher temperature. In the specific case of malonic acid, this shear motion of the chains is so extensive that the cyclic dimers of neighboring chains end up facing each other in the high-temperature α phase (Fig. 2). This process can be visualized by setting in the low-temperature γ phase all angles orthogonal (as in the orthorhombic α phase).

The phase transition of adipic acid at $T_c \simeq 136$ K (Srinivasa Gopalan *et al.*, 1999, 2000) is the only other phase transition in the aliphatic dicarboxylic acids for which structural data are available. The transition comprises part of the same mechanism: torsional relaxation, followed by a substantial translation along the chain axis. In the lower-temperature phase, as with the γ malonic acid phase, we also find two symmetrically independent molecular chains, which upon heating through the transition become equivalent.

Besides temperature, another thermodynamic variable that can be used to chart the conformational energy landscape is pressure. It is increasingly being used to explore this landscape in small organic molecules (*e.g.* Dawson *et al.*, 2005; Boldyreva *et al.*, 2005). Powders of malonic acid were submitted to pressures in excess of 3 GPa; however, no phase transition was detected in this pressure range (Beukes & Weber, 2004)

This work was carried out at Brookhaven National Laboratory under contract DE-AC02-76CH00016 with the US Department of Energy and supported by its Office of Basic Energy Sciences. The work performed at the Swiss Federal Institute of Technology, Lausanne, was supported by a grant from the Tisserand Foundation, Montricher. We are grateful to the late Mr Joseph Henriques for technical assistance. We thank Dr Srinivasa Gopalan and Professor G. U. Kulkarni, Bangalore, for detailed structural information on lower dicarboxylic acids and Professor Emily F. Maverick, Los Angeles, for a copy of THMA11.

References

Becker, P. J. & Coppens, P. (1974). *Acta Cryst.* A**30**, 129–147.
Bernstein, J. (2002). *Polymorphism in Molecular Crystals.* Oxford: Clarendon Press.
Beukes, J.-A. & Weber, H.-P. (2004). Unpublished.
Beyer, T., Lewis, T. & Price, S. L. (2001). *CrystEngComm*, **44**, 1–35.
Boldyreva, E. V., Ivashevskaya, S. N., Sowa, H., Ahsbahs, H. & Weber, H.-P. (2005). *Z. Kristallogr.* **220,** 50–57.

Bond, A. D., Edwards, M. R. & Jones, W. (2001*a*). *Acta Cryst.* E**57**, o141–o142.

Bond, A. D., Edwards, M. R. & Jones, W. (2001*b*). *Acta Cryst.* E**57**, o143–o144.

Bougeard, D., Villepin, J. & Novak, A. (1988). *Spectrochim. Acta A*, **44**, 1281–1286.

Brandenburg, K. (2007). *DIAMOND*. Crystal Impact GbR, Bonn, Germany.

Bürgi, H. B. (2000). *Ann. Rev. Phys. Chem.* **51**, 275–296.

Craven, B. M. & Weber, H.-P. (1983). *Acta Cryst.* B**39**, 743–748.

Craven, B. M., Weber, H.-P. & Klooster, W. T. (1991). *NOOT*, Technical Report. Department of Crystallography, University of Pittsburgh, PA, USA.

Dawson, A., Allan, D. R., Belmonte, S. A., Clark, S. J., David, W. I. F., McGregor, P. A., Parsons, S., Pulham, C. R. & Sawyer, L. (2005). *Cryst. Growth Des.* **5**, 1415–1427.

Delaplane, R. G., David, W. I. F., Ibberson, R. M. & Wilson, C. C. (1993). *Chem. Phys. Lett.* **201**, 75–78.

Delgado, F. S., Hernández-Molina, M., Sanchez, J., Ruiz-Pérez, C., Rodriguez-Martin, Y., López, T., Lloret, F. & Julve, M. (2004). *CrystEngComm*, **6**, 106–111.

Derbyshire, W., Gorvin, T. C. & Warner, D. (1969). *Mol. Phys.* **17**, 401–407.

Derissen, J. L. & Smith, P. H. (1974). *Acta Cryst.* B**30**, 2240–2242.

Desiraju, G. R. (1996). *Acc. Chem. Res.* **29**, 441–449.

Desiraju, G. R. (2007). *CrystEngComm*, **9**, 91–92.

Dunitz, J. D. & White, D. N. J. (1973). *Acta Cryst.* A**29**, 93–94.

Dupré La Tour, M. F. (1932). *Ann. Phys.* **18**, 199–284.

Edwards, M. R., Jones, W. & Motherwell, W. D. S. (2002). *Cryst. Eng.* **5**, 25–36.

Eijck, B. P. van (2002). *J. Comput. Chem.* **23**, 456–462.

Fukai, M., Matsuo, T. & Suga, H. (1991). *Thermochim. Acta*, **183**, 215–243.

Fukushima, K., Watanabe, T. & Umemura, M. (1986). *J. Mol. Struct.* **146**, 61–69.

Ganguly, S., Fernandes, J. R., Desiraju, G. & Rao, C. N. R. (1980). *Chem. Phys. Lett.* **69**, 227–229.

Gao, Q., Weber, H.-P., Craven, B. M. & McMullan, R. K. (1994). *Acta Cryst.* B**50**, 695–703.

Goedkoop, J. A. & MacGillavry, C. H. (1957). *Acta Cryst.* **10**, 125–127.

Hibino, M., Sumi, A., Tsuchiya, H. & Hatta, I. (1998). *J. Phys. Chem. B*, **102**, 4544–4547.

Higgs, P. W. (1953). *Acta Cryst.* **6**, 232–241.

Housty, J. & Hospital, M. (1966*a*). *Acta Cryst.* **20**, 325–329.

Housty, J. & Hospital, M. (1966*b*). *Acta Cryst.* **21**, 29–34.

Housty, J. & Hospital, M. (1967). *Acta Cryst.* **22**, 288–295.

Jagannathan, N. R. & Rao, C. N. R. (1987). *Chem. Phys. Lett.* **140**, 46–50.

Johnson, C. K. (1976). *ORTEP*II, Report ORNL-5138. Oak Ridge National Laboratory, Tennessee, USA.

Johnson, C. K. (1980). *Computing in Crystallography*, edited by R. Diamond, S. Ramaseshan & K. Venkatesan. Bangalore: Indian Academy of Science.

Johnson, C. K. & Levy, H. (1974). *International Tables for X-ray Crystallography*, Vol. IV, p. 316. Birmingham: Kynoch Press.

Kay, M. I. & Katz, L. (1958). *Acta Cryst.* **11**, 289–294.

Kearley, G. J., Fillaux, F., Baron, M.-H., Bennington, S. & Tomkinson, J. (1994). *Science*, **264**, 1285–1289.

Klooster, W. T., Elcombe, M. M. & Weber, H.-P. (2008). In preparation.

Koester, L. (1977). *Springer Tracts in Modern Physics*, Vol. 80, *Neutron Physics*, edited by G. Höhler, p. 36. Berlin: Springer.

Koetzle, T. F. & McMullan, R. K. (1980). Research Memo C-4. Brookhaven National Laboratory.

Krzystek, J., Kwiram, A. B. & Kwiram, A. L. (1995). *J. Phys. Chem.* **99**, 402–409.

Leiserowitz, L. (1976). *Acta Cryst.* B**32**, 775–802.

Leviel, J.-L., Auvert, G. & Savariault, J.-M. (1981). *Acta Cryst.* B**37**, 2185–2189.

Lundgren, J.-O. (1982). *UPALS.* Report UUICB13-4–05. Institute of Chemistry, University of Uppsala, Sweden.

Luo, J., Ruble, J. R., Craven, B. M. & McMullan, R. K. (1996). *Acta Cryst.* B**52**, 357–368.

MacGillavry, C., Hoogschagen, G. & Sixma, F. L. J. (1948). *Rec. Trav. Chim. Pays Bas*, **67**, 869–883.

Maçôas, E. M. S., Fausto, R., Lundell, J., Pettersson, M., Khriachtchev, L. & Räsänen, M. J. (2000). *J. Phys. Chem. A*, **104**, 11725–11732.

McCalley, R. C. & Kwiram, A. L. (1970). *Phys. Rev. Lett.* **24**, 1279–1282.

McCalley, R. C. & Kwiram, A. L. (1993). *J. Phys. Chem.* **97**, 2888–2903.

Meier, B. H., Graf, F. & Ernst, R. R. (1982). *J. Chem. Phys.* **76**, 767–774.

Merchán, M., Tomás, F. & Nebot-Gil, I. (1984). *J. Mol. Struct.* **109**, 51–60.

Meulenaer, J. de & Tompa, H. (1965). *Acta Cryst.* **19**, 1014–1018.

Morrison, J. D. & Robertson, J. M. (1949). *J. Chem. Soc.* pp. 1001–1008.

Rao, C. N. R., Natarajan, S. & Vaidhyanathan, R. (2004). *Angew. Chem. Int. Ed.* **43**, 1466–1496.

Ruiz-Pérez, C., Rodriguez-Martin, Y., Hernández-Molina, M., Delgado, F. S., Pasán, J., Sanchiz, J., Lloret, F. & Julve, M. (2003). *Polyhedron*, **22**, 2111–2123.

Schomaker, V. & Trueblood, K. N. (1998). *Acta Cryst.* B**54**, 507–514.

Srinivasa Gopalan, R., Kumaradhas, P. & Kulkarni, G. U. (1999). *J. Solid State Chem.* **148**, 129–134.

Srinivasa Gopalan, R., Kumaradhas, P., Kulkarni, G. U. & Rao, C. N. R. (2000). *J. Mol. Struct.* **521**, 97–106.

Tao, F., Goswami, J. & Bernasek, S. L. (2006). *J. Phys. Chem. B*, **110**, 4199–4206.

Tarakeshwar, P. & Manogaran, S. (1996). *J. Mol. Struct.* **362**, 77–99.

Taylor, R. & Kennard, O. (1982). *J. Am. Chem. Soc.* **104**, 5063–5070.

Templeton, L. K. & Templeton, D. H. (1973). *Abstr. Am. Cryst. Assoc. Meet.* Storrs, CT, p. 143.

Villepin, J., Novak, A. & Bougeard, D. (1982). *Chem. Phys.* **73**, 291–293.

Weber, H.-P., Craven, B. M. & McMullan, R. K. (1983). *Acta Cryst.* B**39**, 360–366.

Weber, H.-P., Craven, B. M., Sawzik, P. & McMullan, R. K. (1991). *Acta Cryst.* B**47**, 116–127.